Chapter 1
Bugs on a slippery plane
Understanding the motility of microbial pathogens with mathematical modelling

Dmitri O. Pushkin and Martin A. Bees

Abstract Many pathogenic microoranisms live in close association with surfaces, typically in thin films that either arise naturally or that they themselves create. In response to this constrained environment the cells adjust their behaviour and morphology, invoking communication channels and inducing physical phenomena that allow for rapid colonisation of biomedically relevant surfaces or the promotion of virulence factors. Thus it is very important to measure and theoretically understand the key mechanisms for the apparent advantage obtained from swimming in thin films. We discuss experimental measurements of flows around a peritrichously flagellated bacterium constrained in a thin film, derive a simplified mathematical theory and Green's functions for flows in a thin film with general slip boundary conditions, and establish connections between theoretical and experimental results. This article aims to highlight the importance of mathematics as a tool to unlock qualitative mechanisms associated with experimental observations in the medical and biological sciences.

Key words: Flowfields; thin-film flow; microorganisms; biofilms; mathematical modelling

---

Dmitri O. Pushkin
Department of Mathematics, University of York, YO10 5DD, UK e-mail: mitya.pushkin@york.ac.uk

Martin A. Bees
Department of Mathematics, University of York, YO10 5DD, UK e-mail: martin.bees@york.ac.uk

1.1 Introduction

Single-celled microorganisms such as bacteria and algae live in microscopic fluid environments where frictional forces dominate and inertia is negligible. As individuals they employ a range of techniques to move planktonically in fluid or in close association with a surface (Harshey, 2003), ranging from swimming with flagella or body deformations (Turner *et al.*, 2000), to gliding by extending and contracting pili (twitching; Skerker & Berg, 2001), or otherwise, such as propulsion using directed exudate. By swimming or attempting to swim they generate intricate fluid flow structures that are affected by and influence the orientation and motion of other swimming cells.

Frequently and fruitfully microorganisms are found to colonise surfaces, where they are able to exert a measure of control over their local environment with a subtle balance of growth, organisation and expansion. These dynamics are coupled to nutrient availability, signal-molecule mediated intercellular communication, extracellular secretions and the biophysics of interfaces and contact lines (Bees *et al.*, 2000). As a colony they may swim in an existing surface film, forming diffusive rings, or make use of signal molecules, surfactants and wetting agents to expand the perimeter of a thin fluid drop on a surface. Many of these regulatory pathways give rise to or are implicated in biofilm formation, when cells (mono- or multi-species) adhere to one another and to a surface (Verstraeten *et al.*, 2008). Generally, cells in a biofilm are embedded within a structure of extracellular polymeric substance (EPS; mostly proteins, polysaccharides and DNA) that they produce. Biofilms are as important as they are ubiquitous, having the potential to resist anti-microbial treatment whilst expressing virulence factors.

Therefore, it is of fundamental importance to study the physical mechanisms for surface colonisation, swimming in a constrained environment and the earliest stages of biofilm formation. To this end we introduce a simple mathematical model of flows due to swimming in a thin film. While similar modelling is standard in the fluid dynamics literature, we do not know of its application to the motility of microorganisms.

1.2 The need for mechanistic mathematical modelling

Modelling can provide a means to test mechanistic understanding of a biological or physical system not easily accessible with experiments. It is most advantageous when there is a close marriage of experiment and theory such that quantitative or qualitative predictions can be made based on experimental data and tested. In most cases there are no valid models, only models that are good enough to explain the phenomena at hand without having so many unmeasured or unmeasurable free parameters that any behaviour can be fitted, a concept closely related to that of Occam's razor. Thus simplification

is prerequisite to any successful theory, especially in the biological sciences where the complexity can quickly become excessive, obscuring the wood for the trees.

The equations of fluid dynamics are immensely successful, describing flows in fluids (including gases) across many spatial and temporal scales with no free parameters. There application to modelling swimming microorganims is of much recent interest (Lauga & Powers, 2009) as are the measurement of flows around cells, planktonic (Guasto *et al.*, 2011) and sessile (Cisneros *et al.*, 2008). However, their swimming apparatus can be complex, consisting, for example, of multiple interacting helical or plane-wave flagella. Hence, simplification is not only necessary to obtain analytical or computational solutions but desirable for clarity of the mechanisms.

The aim of this article is to provide a minimal model of swimming in a constrained environment that can be employed analytically, rather than a highly complicated description incorporating many features of the morphology of the microorganism that would necessitate complex numerical investigation. We will show that due to its simplicity it provides an insight into the highly nontrivial structure of flowfields around microorganisms observed in experiments (Cisneros *et al.*, 2008; Guasto *et al.*, 2011).

1.3 Morphology

Of significance to this article is the swimming of microorganims in preexisting thin-films. The response of microorganisms to their environment, such as due to the availability of nutrients, via quorum sensing, cell specialisation and spatial self-organisation, are fundamentally different for planktonic cells suspended in a liquid medium than for cells inhabiting wet surfaces and liquid films (Donlan, 2002). This is particularly true for motile cells that swim using flagella (Harshey, 2003).

A striking example is the change in cell morphology when bacteria grow within a wet surface colony. For example, the bacterium *Vibrio parahaemoliticus* (found in saltwater and capable of causing gastroenteritis in humans) grows longer and sprouts many long lateral flagella in addition to the polar flagellum used for swimming in liquid medium (McCarter, 1999). This transformation is orchestrated with the production of extra-cellular surfactants and wetting-agents that allow it to develop a new type of collective motility, swarming, and to form differentiated multicellular communities. Remarkably, most bacterial cells capable of swarming, such as *Echerichia*, *Salmonella*, *Proteus* and *Serratia spp.*, undergo similar (reversible) morphological changes to form elongated, aseptate, mutlinucleated, hyperflagellated cells. This remarkable fact seems to suggest that a distinct evolutionary advantage must be conferred by such morphology on cells inhabiting wet surfaces and films. There is no doubt that longer and more numerous flagella are capable of

creating stronger flows in films. However, swarming cells cannot exert sufficient force to counteract surface tension or contact line dynamics, instead they change the physics with wetting-agents and surfactants that can even allow for rapid (even exponential) expansion of the colony radius (Bees *et al.*, 2002). However, the swimming characteristics of the individuals do have an effect: the morphology of a cell can induce complex flow fields, especially in constrained environments, and collective motion can arise (e.g. Sokolov *et al.*, 2007) potentially adjusting effective mechanical properties of the suspension and influencing fluid-substrate interactions and dipersion of signal molecules.

The enormous medical impact of thin-film infections of pathogenic bacteria, such as *Pseudomonas aeruginosa* and *Staphylococcus aureus*, is long-established and well-documented (Costerton *et al.*, 1999). These and many other bacteria are responsible for lung and airway infections, and nosocomial and catheter-associated bloodstream infections. Typically, the pathogens initially are associated with surfaces, living within a thin film of fluid upon a solid substrate. The upper boundary may be either a liquid-air or liquid-liquid interface. In such a system it is important to disentangle coupled biological and physical mechanisms for the establishment of biofilms; fluid flow around one or more stuck cells may entrain other cells in the vicinity and allow for sufficiently high local concentrations to upregulate quorum sensing activity.

The investigation of swimming within thin-films may also have application in other areas, such as biofuels, where an efficient exchange of gases between the suspension and the air is desirable.

1.4 Measuring the flowfield

Whilst there have been many numerical studies of the interaction between swimming micro-organisms there are only a few measurements. Drescher *et al.* (2010*b*) measured the three-dimensional mean flow around freely-swimming cells of *Chlamydomonas reinhardtii* and *Volvox carterii*, averaged over many flagella beats and cells. They found the expected far-field stresslet (force-dipole) behaviour in three-dimensions, with the magnitude of the velocity decaying approximately as the reciprocal of the radius squared for a buoyant free-swimmer, and Stokelet behaviour (a point force), reciprocal of the radius, for a negatively buoyant swimmer. Guasto *et al.* (2011) extended these results by measuring the flow around freely-swimming cells of *Chlamydomonas reinhardtii*, temporally resolving the flow as it conducts its 50 Hz flagellar beat. They performed these experiments in a pseudo-two-dimensional flow in a film with two stress-free boundaries (a bubble), revealing the complexities of the near-field flows. These flows can be compared with flow fields from numerical computations (O'Malley & Bees, 2012). Drescher *et al.* (2010*a*) measured the flow around freely-swimming bacteria. These studies again revealed stresslet behaviour in the far-field (decaying approximately as the

reciprocal of the radius squared) although they reported the overwhelming importance of stochastic effects in cell-cell and cell-boundary interactions over larger distances.

However, prior to these articles Cisneros *et al.* (2008) measured an altogether different flow for bacteria constrained in thin films between a no-slip and stress-free boundary, as depicted in Figure 1.1d, in contrast to what they observed for freely-swimming cells. One might expect that cells would generate a flow reminiscent of a point force singularity due to the bundled flagella pushing against frictional forces due to the no-slip boundary, especially in the far field. Yet this was not what was observed. Instead, the dominant flow over the observable range was one that rotated about the cell in the plane of the film.

Experimental methods: Liquid cultures of *Bacillus subtilis* 1085B were grown in Ezmix Terrific Broth (TB) for 18 h in a shaker bath at 37 °C and then a 1:50 dilution was prepared in TB and left for an additional 5 h (see Cisneros *et al.*, 2008 for full culture details). This process induced the formation of long, healthy motile cells (typically 4 μm x 0.8 μm). After a further 1:100 dilution with TB, carboxylate-modified 0.21 μm microspheres (Molec. Probes: F8809 - FluoSpheres) were added to act as tracer particles so that the fluid velocity could be observed. A drop of the suspension was placed upon a cover slip that was glued to the outside of a square aperture cut into the base of a Petri dish. A water reservoir and lid eliminated potential for evaporative flows. The drop wetted the surface and fluid was removed by pipette to leave a thin layer of cells. (Not all cover slips allowed thin films to persist; dewetting occurs for some glassware.) Some motile cells swam into shallow regions near the contact line and became wedged between the upper and lower boundaries (several body lengths from the contact line) in a film depth of approximately 1 μm. See Cisneros *et al.* (2008) for more experimental details. Figure 1.1 illustrates the method to extract the flow field using PIV: 1.1a is one frame out of 1500 (at 60 fps) with a (large) cell body and (small) tracer particles; 1.1b demonstrates that the flow is mostly close to the cell body by plotting simply the minimum value at each pixel over 30 frames; 1.1c uses PIV (ImageJ plugin, Q. Tseng) to generate the flowfield; 1.1d presents reprocessed data used in Cisneros *et al.* (2008) with streamlines. These authors report 25 observations of rotating flows from 27 isolated and wedged cells. Cisneros *et al.* (2008) also present data for the much smaller non-rotating flow around freely-swimming cells.

Discussion of experimental results: Clearly, the results indicate that the flow rotates around the mostly stationary cells (the cells rotate stochastically by a couple of degrees about their mean orientations over the course of each experiment). Moreover, it is apparent that the typically 10 μm long flagella are not bundled in any particular orientation. Cisneros *et al.* (2008) argue that the rotating flagella interact more strongly with the lower no-slip boundary than the upper stress-free boundary leading to flagella wrapping around the cell, forming a continuously evolving envelope and driving ro-

tating flow in the plane of the film. A conclusion supported by the absence of rotation when the boundaries are symmetric. Furthermore, one can measure the magnitude, U, of the flow over several directions as a function of distance, r, from the cell (in μm, units of the cell diameter or units of film thickness). Surprisingly, Cisneros *et al.* (2008) find that the flow decays over a couple of body lengths (10 body widths) as $U \propto e^{-kr}$, where $k \approx \frac{1}{4}\ \mu\text{m}^{-1}$, in stark contrast to the expected logarithmic or reciprocal decay expected of a point force in two or three dimensional non-constrained flow, respectively. This observation should be explained.

1.5 Mathematics of modelling swimming in a thin film

In this section, we shall describe some approximations and solutions for swimming cells in thin-films. Mathematically inclined readers will discover in this section that swimming in a constrained environment in a thin-film that allows for asymmetry in the boundary conditions leads to near field behaviour that is distinct from swimming in simple two-dimensional or three-dimensional fluid. The transition between near and far-field effects will be explored. Mathematically disinclined readers can skip this section in favour of the discussion of results and comparison with experiments in Section 1.6.

For simple fluids at low Reynolds number the fluid motion is governed by the Stokes equations, a set of linear equations that possess a time-reversal symmetry. The implication in this microscopic environment is that to move cells need adopt a swimming stroke that looks different when played in reverse (allowing for an arbitrary strictly-increasing nonlinear scaling of time).

Many biological fluids have complex viscoelastic and rheological properties (mucus, blood, etc.). Here, however, we consider the simplest case of a Newtonian fluid with viscosity μ (i.e. we assume that the fluid possess negligible viscoelasticity). We assume the film to be infinite and flat and to have a constant thickness h. Furthermore, and significantly, we assume the film to be thin. This assumption means that flows generated by swimmers quickly become (quasi) two-dimensional at distances r much larger than h, such that $r \gg h$.

Boundary conditions at small spatial scales can be complex. For microscopic scales a no-slip condition is commonly used. However, biological and complex fluids often show significant apparent slip in a variety of situations, e.g. when polymers dissolved in the fluid are poorly adsorbed by the wall, or the wall-adsorbed polymer chains undergo a stretch-coil transition (Lauga *et al.*, 2007). Other factors leading to a significant slip include surface roughness, hydrophobicity, electric charge and dissolved gases (Tretheway & Meinhart, 2002; Zhu & Granick, 2002; Lauga *et al.*, 2007). Therefore, we employ a general *slip* boundary condition at the bottom and the top of the film, such that

$$\mathbf{v} - l\frac{\partial \mathbf{v}}{\partial n} = 0, \tag{1.1}$$

where $\mathbf{v}$ is the (three-dimensional) fluid velocity, the derivative is taken along the normal to the film boundary with coordinate n and the slip length l may be different for the top and the bottom film boundaries. For $l = 0$ this boundary condition corresponds to the *no-slip* condition requiring that the fluid velocity vanishes on a fluid-solid interface; for $l = \infty$ the condition describes a stress-free interface. Intermediate values of l are typical for fluid-fluid interfaces. For example, if another fluid layer is sandwiched between the film and the solid substrate $l \sim h_1\mu/\mu_1$, where μ_1 and h_1 are the viscosity and the thickness of the sandwiched fluid layer.

Within the thin film approximation the velocity component normal to the film is negligible, and it can be shown that the two-dimensional fluid velocity $\mathbf{u}(x, y)$, defined as the local velocity $\mathbf{v}$ averaged over the film thickness, is governed by

$$-\nabla p + \mu\nabla^2\mathbf{u} - \kappa\mathbf{u} = 0, \tag{1.2}$$

where $p(x, y)$ is the fluid pressure and κ is the local friction coefficient. While the first two terms describing the balance of the pressure and viscous stresses between neighbouring layers of fluid are identical to the terms of the Stokes equation, the last term describes the damping effect of the film boundaries. The local friction coefficient can be related to the film thickness and the slip lengths l_1 and l_2 at the bottom and the top of the film, respectively:

$$\kappa = \mu/\lambda^2, \quad \lambda^2 = \frac{h\left(h^2 + 4h(l_1 + l_2) + 12l_1l_2\right)}{h + l_1 + l_2}. \tag{1.3}$$

In particular, for a channel that is formed by two parallel solid planes with no-slip boundary conditions (a Hele-Shaw cell) $\lambda = h$. For a stress-free top boundary $\lambda = 2\sqrt{h\,(h + 3l_1)}$. If, in addition, the bottom boundary is no-slip then $\lambda = 2h$; alternatively, if $l_1 \gg h$, then $\lambda = 2\sqrt{3hl_1}$. Equation (1.2) should be supplemented by the fluid incompressibility condition

$$\nabla \cdot \mathbf{u} = 0. \tag{1.4}$$

The thin-film flow generated by a point force $\mathbf{F}$ applied at the origin must satisfy

$$-\nabla p + \mu\nabla^2\mathbf{u} - \kappa\mathbf{u} = -\rho\mathbf{F}\delta(\mathbf{r}), \tag{1.5}$$

where $\mathbf{r}$ is the position vector and ρ is the fluid density. It turns out that the exact solution of (1.4) and (1.5) can be found analytically, such that

$$\mathbf{u_f}(\mathbf{r}, \mathbf{F}) = \mathbf{G_f} \cdot \frac{\mathbf{F}}{2\pi\nu}, \quad \mathbf{G_f} = f_1(r/\lambda)\mathbf{I} + f_2(r/\lambda)\hat{\mathbf{r}}\hat{\mathbf{r}}, \tag{1.6}$$

$$f_1(x) = K_0(x) - \left(x^{-2} + x^{-1}K_0'(x)\right), \tag{1.7}$$

$$f_2(x) = 2x^{-2} - x\left(x^{-1}K_0'(x)\right)', \tag{1.8}$$

where $\nu = \mu/\rho$ is the kinematic viscosity of the fluid, $\mathbf{I}$ is the identity tensor, $r = \|r\|$, $\hat{\mathbf{r}} = \mathbf{r}/r$ and $K_0(x)$ is the modified Bessel function of the second kind. As the governing equations are linear, this solution may be used to construct arbitrary (quasi-two-dimensional) flows in thin films using the Green's functions formalism (Pozrikidis, 1992). Therefore, we will refer to $\mathbf{u_f}$ as the Green's function for a thin film slip flow.

In order to understand this solution, let us first consider its asymptotes:

$$x \to 0: \quad f_1 \sim \frac{1}{2}\ln(2x^{-1}) - \gamma,\ f_2 \sim \frac{1}{2}; \tag{1.9}$$

$$x \to \infty: \quad f_1 \sim -x^{-2},\ f_2 \sim 2x^{-2}. \tag{1.10}$$

Here, $\gamma \approx 0.577$ is the Euler constant. The first asymptote describes the flow generated by a concentrated force at length scales much less than the slip length λ, $r \ll \lambda$. Hence,

$$\mathbf{u_f} \approx \mathbf{u}_{\text{free}} = \left[\left(\ln\frac{2\lambda}{r} - \gamma\right)\mathbf{I} + \hat{\mathbf{r}}\hat{\mathbf{r}}\right] \cdot \frac{\mathbf{F}}{4\pi\nu}, \quad r \ll \lambda. \tag{1.11}$$

The Green's function $\mathbf{u}_{\text{free}}$ describes hydrodynamic interactions in a film with no friction at the film boundaries. The structure of this flow is presented in Figure 1.2a.

The expression $\mathbf{u}_{\text{free}}$ can be obtained directly from the Stokes equations (i.e. equation (1.2) with $\kappa = 0$; Pozrikidis, 1992) in two dimensions. Note that the first term in the brackets contains a logarithm, which diverges for $r \to 0$ and $r \to \infty$. The short-distance divergence is natural as we assume a point force; in real flows it will be cured by the finite size of the microorganism. The large-distance divergence is a signature of the *Stokes paradox*, which is explicitly resolved here by the requirement $r \ll \lambda$; the (weak) dependence of the argument of the logarithm on λ remains its only vestige. The Green's function analogous to $\mathbf{u}_{\text{free}}$ has been used recently to quantify hydrodynamic interactions in free fluid films (Di Leonardo *et al.*, 2008); note, however, that we obtain somewhat different numerical values for constants in the pre-factor of $\mathbf{I}$ in (1.11).

The asymptote 1.10 describes the flow produced by a concentrated force far beyond the slip length λ, yielding

$$\mathbf{u} \approx \mathbf{u}_{SD} = -\frac{1}{r^2}\left[\mathbf{I} - 2\hat{\mathbf{r}}\hat{\mathbf{r}}\right] \cdot \frac{\rho}{\kappa}\frac{\mathbf{F}}{2\pi}, \quad r \gg \lambda. \tag{1.12}$$

This flow can be obtained as the balance of the friction force at the boundaries and the pressure, which enforces incompressibility of the fluid. Importantly, this flow can be re-written as

$$\mathbf{u}_{SD} = -2\nabla\nabla\ln r \cdot \frac{\lambda^2\mathbf{F}}{4\pi\nu}, \tag{1.13}$$

which means that this singular flow can be considered as a two-dimensional source doublet flow (Pozrikidis, 1992). Figure 1.2 shows the streamlines of this flow. Notably, the streamlines form closed loops. For a film with no-slip boundaries $\lambda = h$; this particular source doublet flow has been used recently to describe flows created in Hele-Shaw cells by microorganisms and by moving droplets (e.g. see Pepper *et al.*, 2009; Brotto *et al.*, 2013). We predict that the effect of fluid slip at large distances is the enhancement of the source dipole strength by the factor of $(\lambda/h)^2$.

Thus, the flow $\mathbf{u_f}$ has a very different structure for $r \ll \lambda$ and $r \gg \lambda$. The structure of the full flow is shown in Figures 1.2c,d using the system of units with $\lambda = 1$. The region dominated by the logarithmic singularity continuously merges with the recirculatory flow region. This picture illustrates the utility of the Green's function $\mathbf{u_f}$, which may be used to describe thin film flows in the whole domain.

Finally, we would like to comment on the behaviour of the fluid vorticity in slip flows. By contrast with the Stokes equations, for which the vorticity diffuses infinitely fast throughout the fluid (Acheson, 2002), the vorticity in thin film flows with slip boundary conditions can diffuse only a distance of order λ from the vorticity source. Indeed, taking the curl of (1.2) results in an equation for the (only non-zero) vorticity component normal to the film ω, satisfying

$$\nabla^2\omega - \frac{1}{\lambda^2}\omega = 0. \tag{1.14}$$

Its bounded axisymmetric solution is given by

$$\omega = \text{const} \times K_0(r/\lambda) \sim e^{-r/\lambda}\sqrt{\frac{\lambda}{r}}, \quad r \gg \lambda, \tag{1.15}$$

and the flow circulation around the contour $\|\mathbf{r}\| = r$ varies with distance as

$$\mathit{\Gamma}(r) \sim e^{-r/\lambda}\sqrt{\frac{r}{\lambda}}, \quad r \gg \lambda. \tag{1.16}$$

Hence, the decay of the circulation is approximately exponential.

1.6 Discussion and concluding remarks

Thin film flows are very typical of environments where pathogens are seen to thrive, with rapid colonisation of the film and other tissues, going on to form troublesome antimicrobial resistant biofilms with enhanced virulence. We have described how mathematical modelling can be used as a tool to explore mechanisms behind experimental observations. A proper understanding

of the fluid dynamics and coupling with biological and physical processes will reveal why it is that microorganims gain such an advantage when colonies are associated with surfaces. It is likely that there is not one main reason, but a combination of factors.

We have shown from experimental measurements and mathematical analysis of a simplified fluid system that the flow due to a swimming microorganism in a confined environment, such as within a thin film of fluid can be very different to the flow due to an unconstrained swimmer, particularly when there are asymmetric boundary conditions (e.g. a film on a substrate with a liquid-liquid or liquid-gas upper interface).

We have found a Green's function for a thin film in the presence of two general boundary conditions for the film that is valid over the whole domain. In particular, the results make clear how near-field logarithmic dynamics merge into a recirculatory flow regime. We can tune our slip parameters for symmetric and asymmetric cases (see 1.2), and have observed that the circulation decays exponentially with distance, with a parameter that can relate the slip length to experimental measurements of flow fields.

Finally, it is tempting to consider how the local flows observed in experiments (see Figure 1.1d) could be constructed from the fundamental Green's solutions. In fact, a similar flow arises very naturally. In Figure 1.3 we plot the flowfield due to a force couple, or, in other words, to two forces associated with the principal flagella bundles located either side of a rod-shaped bacterium pointing in opposing directions. The resemblance of Figures 1.1d and 1.3 is striking; each has a region of pinched closed orbits about the body or origin that are clasped between two eddies (at the top and bottom of each picture). Therefore, it would appear that the complex system of a cell with several interacting helical flagella that are attached to the body via a flexible joint in a confined three-dimensional fluid between two general boundaries may be reduced to a system of two point force solutions for an asymptotically equivalent two-dimensional system.

We plan to explore this system further and investigate interactions between swimmers, but for this we need first to consolidate and challenge the mathematical simplification and results with new experiments.

References

Acheson, D. J. 2002 *Elementary fluid dynamics*. Oxford University Press.

Bees, M. A., Andresén, P., E., Mosekilde & Giskov, M. 2000 The interaction of thin-film flow, bacterial swarming and cell differentiation in colonies of *Serratia liquefaciens*. *Journal of Mathematical Biology* **40**, 27–63.

Bees, M. A., Andresén, P., E., Mosekilde & Giskov, M. 2002 Quantitative effects of medium hardness and nutrient availability on the swarming

motility of *Serratia liquefaciens*. *Bulletin of Mathematical Biology* **64**, 565–587.

Brotto, T., Caussin, J.-B., Lauga, E. & Bartolo, D. 2013 Hydrodynamics of confined active fluids. *Physical review letters* **110** (3), 038101.

Cisneros, L. H., Kessler, J. O., Ortiz, R., Cortez, R. & Bees, M. A. 2008 Unexpected bipolar flagellar arrangements and long-range flows driven by bacteria near solid boundaries. *Phys. Rev. Lett.* **101**, 168102.

Costerton, J. W., Stewart, P. S. & Greenberg, E. P. 1999 Bacterial biofilms: A common cause of persistent infections. *Science* **284** (5418), 1318–1322.

Di Leonardo, R, Keen, S, Ianni, F, Leach, J, Padgett, MJ & Ruocco, G 2008 Hydrodynamic interactions in two dimensions. *Physical Review E* **78** (3), 031406.

Donlan, R. M. 2002 Biofilms: microbial life on surfaces. *Emerg. Infect. Dis.* **8** (9).

Drescher, K., Dunkel, J., Cisneros, L. H., Gangulya, S. & Goldstein, R. E. 2010*a* Fluid dynamics and noise in bacterial cell–cell and cell–surface scattering. *Proc. Nat. Ac. Sci. USA* **108** (27), 10940–10945.

Drescher, K., Goldstein, R. E., Michel, N., Polin, M. & Tuval, I. 2010*b* Direct measurement of the flow field around swimming microorganisms. *Phys. Rev. Lett.* **105**, 168101.

Guasto, J. S., Johnson, K. A. & Gollub, J. P. 2011 Measuring oscillatory velocity fields due to swimming algae. *Physics of Fluids.* **23**, 091112.

Harshey, R. M. 2003 Bacterial motility on a surface: Many ways to a common goal. *Annu. Rev. Microbiol.* **57**, 249–73.

Lauga, E., Brenner, M. & Stone, H. 2007 Microfluidics: the no-slip boundary condition. In *Springer handbook of experimental fluid mechanics*, pp. 1219–1240. Springer.

Lauga, E. & Powers, T. R. 2009 The hydrodynamics of swimming microorganisms. *Rep. Prog. Phys.* **72**, 096601, 36pp.

McCarter, L. 1999 The multiple identities of vibrio parahaemolyticus. *Journal of molecular microbiology and biotechnology* **1** (1), 51–57.

O'Malley, S. O. & Bees, M. A. 2012 The orientation of swimming biflagellates in shear flows. *Bulletin of Mathematical Biology* **74**, 232–255.

Pepper, R. E., Roper, M., Ryu, S., Matsudaira, P. & Stone, H. A. 2009 Nearby boundaries create eddies near microscopic filter feeders. *Journal of the Royal Society Interface* **12**, 1–12.

Pozrikidis, C. 1992 *Boundary integral and singularity methods for linearized viscous flow*. Cambridge University Press.

Skerker, J. & Berg, H. C. 2001 Direct observation of extension and retraction of type iv pili. *Proc. Natl. Acad. Sci. USA* **98**, 6901–4.

Sokolov, A., Aranson, I. S., Kessler, J. O. & Goldstein, R. E. 2007 Concentration dependence of the collective dynamics of swimming bacteria. *Phys. Rev. Lett.* **98**, 158102.

Tretheway, D. C. & Meinhart, C. D. 2002 Apparent fluid slip at hydrophobic microchannel walls. *Physics of Fluids* **14**, L9–L12.

Turner, L., Ryu, W. S. & Berg, H. C. 2000 Real-time imaging of fluorescent flagellar filaments. *Journal of Bacteriology* **182** (10), 2793–2801.

Verstraeten, N., Braeken, K., Debkumari, B., Fauvart, M., Fransaer, J., Vermant, J. & Michiels, J. 2008 Living on a surface: swarming and biofilm formation. *Trends Microbiol.* **16**, 496–506.

Zhu, Y. & Granick, S. 2002 Limits of the hydrodynamic no-slip boundary condition. *Physical review letters* **88** (10), 106102.

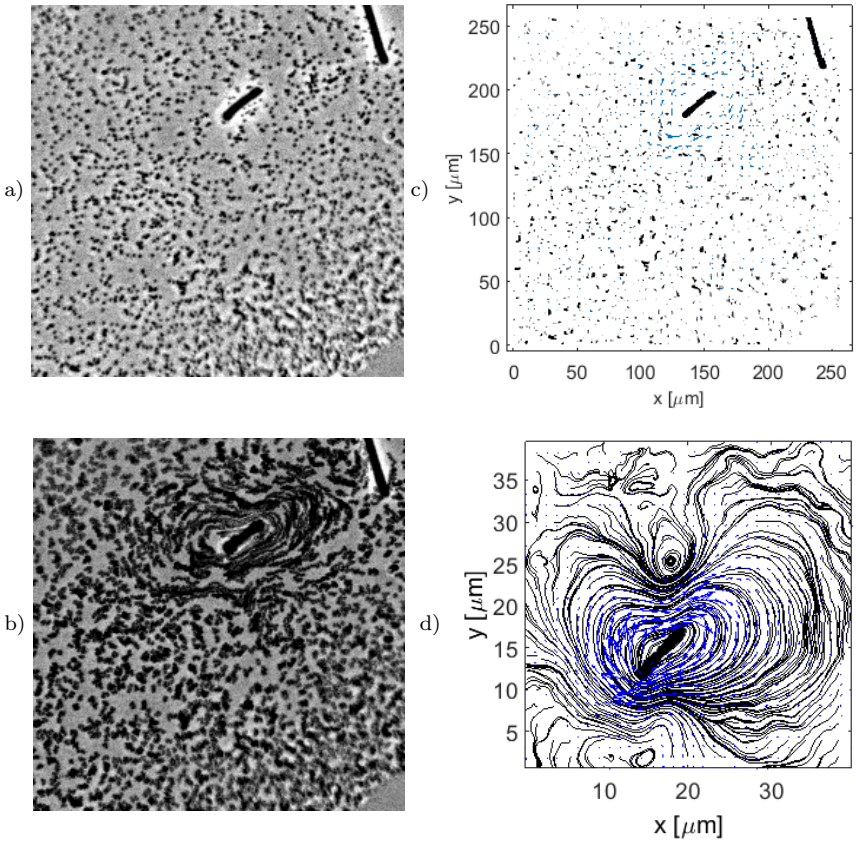

Fig. 1.1: a) One frame of a series of 1500: the large particle is the body (4 μm $\times$ 0.8 μm) of a peritrichously flagellated (6-15 flagella; 10 μm long & 20 nm diameter; 3 μm pitch; rotating at 100 Hz) cell of *Bacillus subtilis*. The small dots are tracer particles of diameter 210 nm, and the resolution is 256 $\times$ 256 pixels. b) A processed image of the minimum value at each pixel over 30 frames (at 60 fps) around a stuck cell of *Bacillus subtilis*: the motion of the tracer particles illustrates the flow around the cell body. c) The arrows indicate the vector field around the stuck cell obtained with PIV (ImageJ plugin, Q. Tseng). The small dots are the tracer particles. d) Streamlines and flowfield vectors about a second cell. [Subfigure d) is replotted, with permission, from data used in Cisneros *et al.*, 2008 using similar methods.]

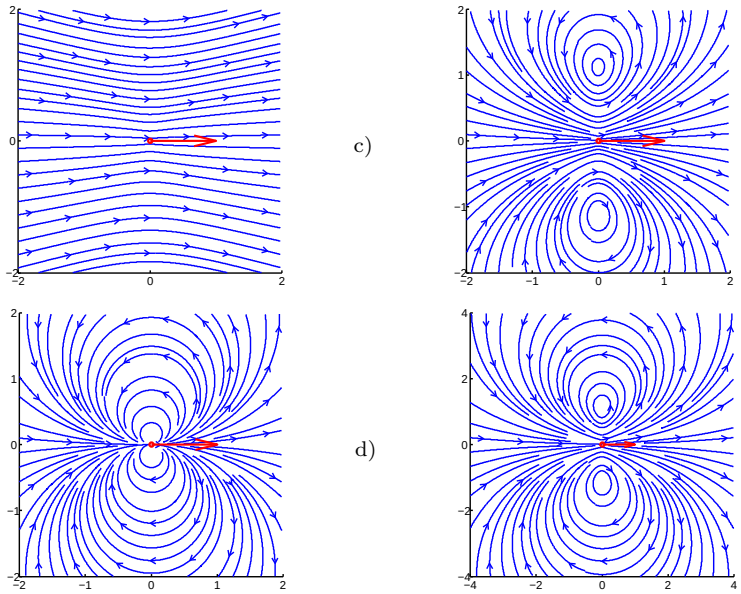

Fig. 1.2: Fluid flows due to a unit point force in thin films with different boundary conditions. The direction of the force is indicated by the unit red arrow. (a) The flow in a free-standing film is unidirectional, dominated by a (weak) logarithmic singularity at $r = 0$. (b) The flow in a film with no-slip boundaries (Hele-Shaw cell) shows characteristic closed-loop streamlines. The structure of the slip flow $\mathbf{u_f}$ (1.6) with $\lambda = 1$ is given in (c) and (d) for the box sizes $L_{box} = 2$ and $L_{box} = 4$, respectively. It is clear that the region dominated by the logarithmic singularity continuously merges with the recirculatory flow region. These figures illustrate the utility of the Green's function $\mathbf{u_f}$, which may be used to describe thin film flows in the whole domain.

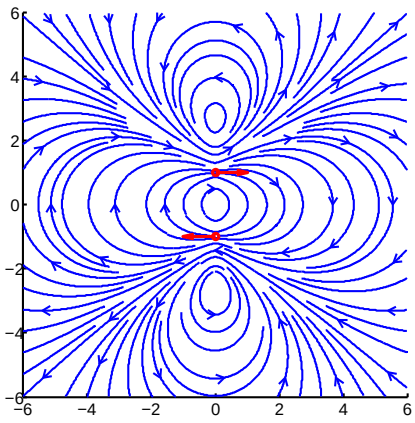

Fig. 1.3: Slip flow in a thin film due to a force couple; two point forces (red arrows) pointing in positive and negative x-directions separated by distance of 2 μm in the y-direction.